June 2026

Quantum mechanical string shoving

Linn Preuss Jelvez

Theoretical Particle Physics
Division of Particle and Nuclear Physics
Department of Physics
Lund University

Master thesis (30 hp) supervised by Christian Bierlich

LUND UNIVERSITY

Abstract

The Lund string model, which is implemented in PYTHIA, describes the hadronization process by representing the color electric field between a $q\bar{q}$ pair as a massless, relativistic string. In the string shoving extension, the strings will have a Gaussian profile and will repel each other when they interact, acting like classical objects. When two strings interact and are positioned perpendicular to the reaction plane, they will produce a negative elliptic flow ($v_2 < 0$), meaning the movement will be along the minor axis of the elliptical interaction region. This thesis explores how the string shoving works in a quantum mechanical treatment. In a simplified quantum model, a collision between two strings is represented as a Gaussian wave packet interacting with a Gaussian potential. The Schrödinger equation is solved in both one and two dimensions to find that the strings move differently than predicted by the Lund string model. The simplified model shows that a large effective potential can suppress mobility of the string away from the interaction region. The radial probability current shows angular broadening, with peak structures appearing in certain parameter regions. However, the numerical robustness of these peaks should be studied further. The elliptic flow, calculated in a toy geometry, shows that the magnitude of v_2 decreases compared to the classical case. The work in this thesis motivates further studies of a quantum mechanical treatment of strings in hadronization.

Populärvetenskaplig beskrivning

Kvarkar bygger upp partiklar vi kan se i experiment. Enligt kvantkromodynamiken kan kvarkar inte leva ensamma, utan kommer att vara bundna till varandra i en sträng. Denna sträng är en samling av energi som kommer att öka när kvarkarna rör sig ifrån varandra, likt ett gummiband som töjs. Dessa strängar är viktiga , och för att förstå hur kvarkar går ihop till hadroner, behöver de studeras noggrant. En sträng kommer att röra sig och töjas tills energin blir stor nog att den går sönder och bildar hadroner. Innan strängar går sönder, kommer de att knuffa varandra och interagera med varandra, och idag finns modeller av dessa strängar och hur de påverkar varandra. En välanvänd modell av hadroniseringen är PYTHIA, som är en Monte-Carlo händelsegenerator som simulerar partikelkollisioner. Denna händelsegenerator är baserad på den fenomenologiska Lund strängmodellen, som antar att strängarna är klassiska objekt. Enligt denna modell kommer strängarna alltid att repellera varandra efter att de kolliderat, precis som att biljardbollar skulle krocka med varandra.

En bra uppfattning av hur strängarna beter sig ger en tydligare bild av processen som är att bilda partiklar som vi senare kan observera i experiment, för att jämföra och säkerställa resultat. Strängarna är extremt små objekt, som gör dom kvantobjekt, och det skulle därför vara logiskt att använda en modell som behandlar dem som kvantobjekt. Det är förväntat att en modell som antar att strängarna är kvantobjekt kommer att förutspå ett annorlunda beteende av strängarna.

När strängar kolliderar kommer kollideringsarean att vara en ellips med en storaxel och en lillaxel. Ett negativt elliptiskt flöde ($v_2 < 0$) innebär att strängarna kommer att röra sig längs lillaxeln, medan $v_2 > 0$ innebär att de rör sig längs storaxeln. Man brukar tro att stora kollisioner bildar kvark-gluon plasma, som ger upphov till ett positivt elliptiskt flöde. Små kollisoner, som kollisioner mellan strängar, visar dock att de kommer att ha ett negativt elliptiskt flöde och motsäger det kvark-gluon plasma förutsäger. Mitt arbete ifrågasätter ifall strängarna kommer att röra sig i andra riktningar om de hanteras som kvantobjekt. Jag har utvecklat en numerisk modell som löser Schrödinger-ekvationen i både en och två dimensioner, och kan bestämma strängarnas position en viss tid efter de kolliderat. Denna kvantmodell säger att strängarna inte längre kommer att röra sig i endast en riktning efter de kolliderar, utan sannolikheten för att röra sig i flera riktnignar är inte noll. Hur de rör sig beror på saker såsom hur nära strängarna är, hur snabbt de rör sig och hur många strängar som är involverade i kollisionen. Resultaten från denna kvantmodell kommer att ge en jämförelse mellan vad det innebär att hantera strängarna som ett klassiskt objekt eller ett kvantobjekt. I jämförelse med experiment bör detta ge en klarare bild av hadronisering och bidra till möjligheten av bättre modeller och experiment i framtiden.

Contents

1 Introduction **4**

2 Theory background **6**
2.1 What is a Lund string 6
2.2 String interactions in the Lund string model 9
2.3 PYTHIA 10
2.4 2-site toy model in QM 10

3 Method **12**
3.1 One-dimensional implementation 12
3.2 Two-dimensional implementation 14
3.3 Near-region probability and probability current 15
3.4 Elliptic flow 16

4 Results **18**
4.1 Lund strings in one dimension 18
4.2 Lund strings in 2D 20
4.3 Interaction at characteristic hadronization time scale 22
4.4 Calculating v_2 26

5 Conclusion **29**

A Full derivation of 2-site model **30**

B Full derivation of the Schrödinger equation in a 2-body system **33**

1 Introduction

Hadronization is the process where quarks and gluons combine to form hadrons that can be observed. PYTHIA [1] is a Monte Carlo [2] event generator used to model this process that simulates collisions between high-energy particles and describes the full event going from an initial interaction to observable particles. In quantum chromodynamics (QCD) the color-electric field between the interacting quarks will be confined into a color-flux tube. PYTHIA uses the Lund string model [3], which treats the color-flux tube as a classical, massless and relativistic string.

The string will stretch as the quarks move further apart from each other, and at some distance the energy in the string will be enough to create a new quark pair. This process happens many times and the string breaking will result in hadrons. In interactions where many final state particles are created, many strings are formed and they will interact with each other. In a dense system, the Lund string model introduces a repulsive force between the strings, resulting in string shoving [4], where the color-electric field of a string has an almost Gaussian profile [5].

When strings collide, the interaction region is elliptic, with a minor and a major axis. A negative elliptic flow ($v_2 < 0$) means that the strings will interact to induce a motion along the minor axis, while a positive elliptic flow means that the strings induce a motion along the major axis after colliding. In heavy-ion collisions, the quark-gluon plasma (QGP) that is formed is expected to have a positive elliptic flow ($v_2 > 0$) [6]. When two strings interact, the overlap area will have a very high energy making it reasonable to assume that the strings should behave as QGP. However, the string shoving model predicts the opposite for the small collisions and says that the elliptic flow will be negative [1][6].

The goal of the thesis is to study how the behaviour of the strings will change if treated quantum mechanically and how it will affect the elliptic flow. When treated quantum mechanically, the strings will no longer only repel each other and the probability to move in any direction can be calculated as a probability distribution over space. The potential energy in the string is proportional to the distance between the quarks. Two strings moving away from each other can be treated as a potential-barrier problem described by the Schrödinger equation, where the relative motion between the strings is given by a Gaussian wave packet. Solving the Schrödinger equation for different initial conditions would give an understanding of how the strings will interact with each other. In a simplified model, a higher potential is taken as a proxy for many strings. The wave packet will be less likely to escape the potential, meaning the strings will be less likely to move away from the interaction region. This is the main idea of this project.

The working hypothesis of this thesis is that a quantum mechanical treatment of string interactions will change the magnitude of v_2. The work in this project is structured as follows. Section 2 explains the necessary theoretical background to understand the results, including strings in the Lund string model and what PYTHIA is. Section 3 explains the methods used to solve the Schrödinger equation in one and two dimensions. It also explains how the radial probability current and elliptic flow are calculated. The next sections contain the results. The string interactions are treated in both one dimension and two dimensions, resulting in probability distributions of the relative position of the strings. Additionally, the probability current is calculated to see how the system evolves over time and in what directions the strings want to move after interacting. The radial probability current is calculated for different distances from the interaction region and different relative momenta. Finally, v_2 is calculated and a comparison to the classical case is made. From these results, a conclusion is made and stated in the last section.

2 Theory background

This section presents the theoretical background necessary to understand the string interactions discussed in the results. It explains how a string is formed and what a string is, highlighting important quantities such as the energy stored in the string and the string tension. The process of string breaking and creating hadrons is then introduced. Furthermore, it is explained how the strings will overlap and interact through the string shoving mechanism. String interactions in the Lund model, including the repelling force between the strings and the average interaction time, are explained. Finally, a 2-site quantum toy model is presented to give an understanding of how the strings are expected to behave in a quantum mechanical picture.

2.1 What is a Lund string

Interactions in quantum chromodynamics (QCD) have two characteristic properties; asymptotic freedom at small distances and confinement at large distances. When a $q\bar{q}$ pair interacts by exchanging gluons, the potential grows linearly at large r, corresponding to an approximately constant confining force with magnitude κ. The exchange of gluons gives rise to a color-electric field, where the potential energy between the quark and antiquark is given by the Cornell potential. The Cornell potential has the form [7]

$$V(r) = -\frac{4\alpha_s}{3r} + \kappa r. \tag{2.1}$$

The first term describes the Coulomb potential that will be dominant at small distances, where α_s is the coupling constant. The second term describes the confining potential that becomes dominant at large distances, r, and increases linearly. κ is a constant of proportionality, which corresponds to the string tension, and will have a value of $\kappa \approx 1$ GeV/fm [5]. The potential between the quarks is shown in Figure 1 and the linear part of the graph is where the Coulomb potential becomes negligible [8].

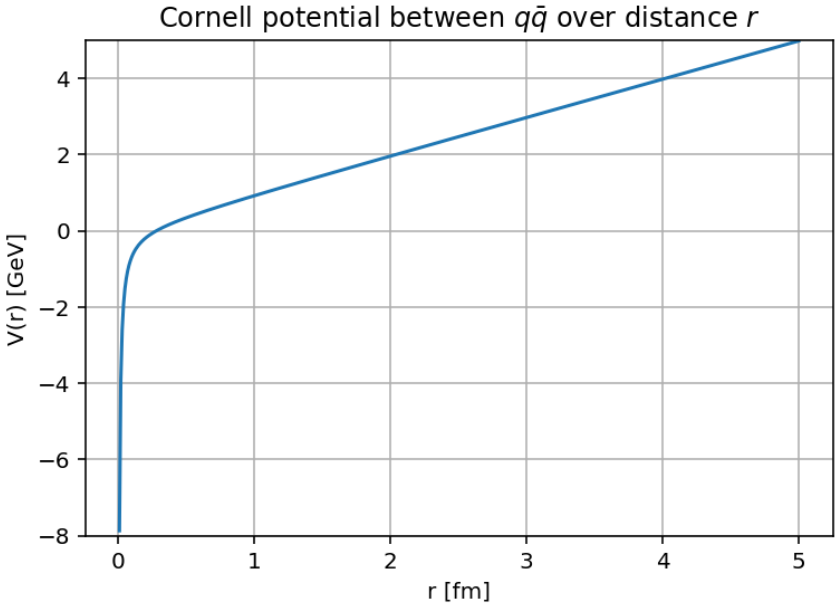

Figure 1: The interaction energy between a $q\bar{q}$ pair as a function of the distance between them. The plot shows the potential for $\kappa = 1$ GeV.

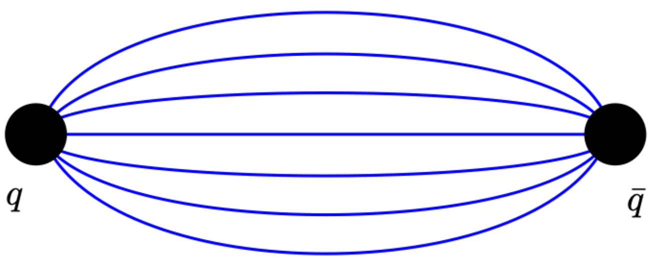

Figure 2: Illustration of the color-electric field between an $q\bar{q}$-pair confined to a color flux tube.

Thus, at large r the color-electric field between the $q\bar{q}$ pair will be confined to a color flux tube and the potential can be approximated as

$$V(r) \approx \kappa r. \tag{2.2}$$

This approximation is used in the Lund string model. The color-electric field becomes confined into a color-flux tube, which is illustrated in Figure 2. In the Lund string model, the color-flux tube is called a string and when the energy stored in the string is large enough to create a new $q\bar{q}$ pair, it will break. To picture the hadronization, the strings can be aligned with the x-axis, and then new $q\bar{q}$ pairs will be produced along the hyperbola.

This is shown in Figure 3. The new quark-pairs are produced and close-by quarks will combine into hadrons, which are depicted as arrows.

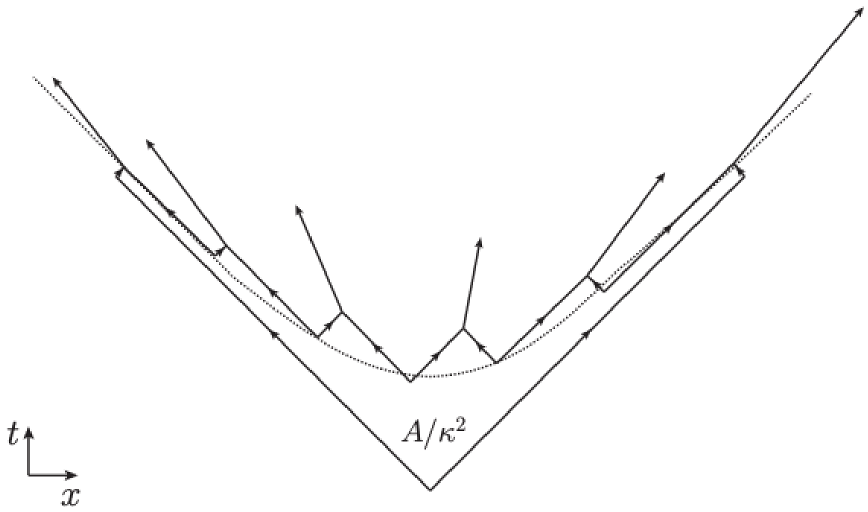

Figure 3: Illustration of a string breaking into hadrons. The new $q\bar{q}$ pairs are produced along a hyperbola and then combine into hadrons, depicted as arrows. Figure taken from ref. [1].

The strings will be able to interact before the hadronization, which happens at time τ. The distribution of string break vertices in proper time is given by

$$\mathcal{P}(\Gamma)d\Gamma = \Gamma^a \exp(-b\Gamma)d\Gamma \quad , \quad \Gamma = (\kappa\tau)^2, \tag{2.3}$$

Here, $\mathcal{P}$ is the probability of a string breaking and creating a new $q\bar{q}$ pair. The transverse momentum and mass of the new quarks are determined by the Gaussian distribution defined as [5]

$$\frac{d\mathcal{P}}{d^2p_\perp} \propto \kappa \exp\left(\frac{-\pi m_{\perp,q}^2}{\kappa}\right), \quad m_\perp^2 = m_q^2 + p_{\perp,q}^2. \tag{2.4}$$

Equation (2.4) describes that the new quarks will get a random transverse momentum kick given by the Gaussian distribution that describes the probability of creating a new quark with the momentum p. The average value of τ is calculated to be

$$\sqrt{\langle\tau^2\rangle} = \sqrt{\frac{1+a}{b\kappa}} \approx 1.41 \text{ fm}. \tag{2.5}$$

The values of a and b are determined from experiments [3]. When the string breaks, each break will give one hadron and each hadron will take away a momentum fraction z from the remaining light-cone momentum. The remaining momentum after one break would be

$(1-z)$ and so on. The distribution of momentum fraction that each hadron takes is given by [5]

$$f(z) \propto \frac{(1-z)^a}{z} \exp\left(-\frac{bm^2}{z}\right), \tag{2.6}$$

where m is the mass of the hadron and the values of a and b are the same values as in Equation (2.5). PYTHIA uses a three-dimensional version of Equation (2.6), where the mass is replaced by the transverse mass [6].

2.2 String interactions in the Lund string model

The Lund string model is a semi-classical model. When the strings interact they are treated as relativistic, classical objects. In lattice QCD, it is possible to calculate the strength of the color-electric field as a function of the transverse distance from the flux tube axis [5]. The results are shown in Figure 4, together with a Gaussian fit.

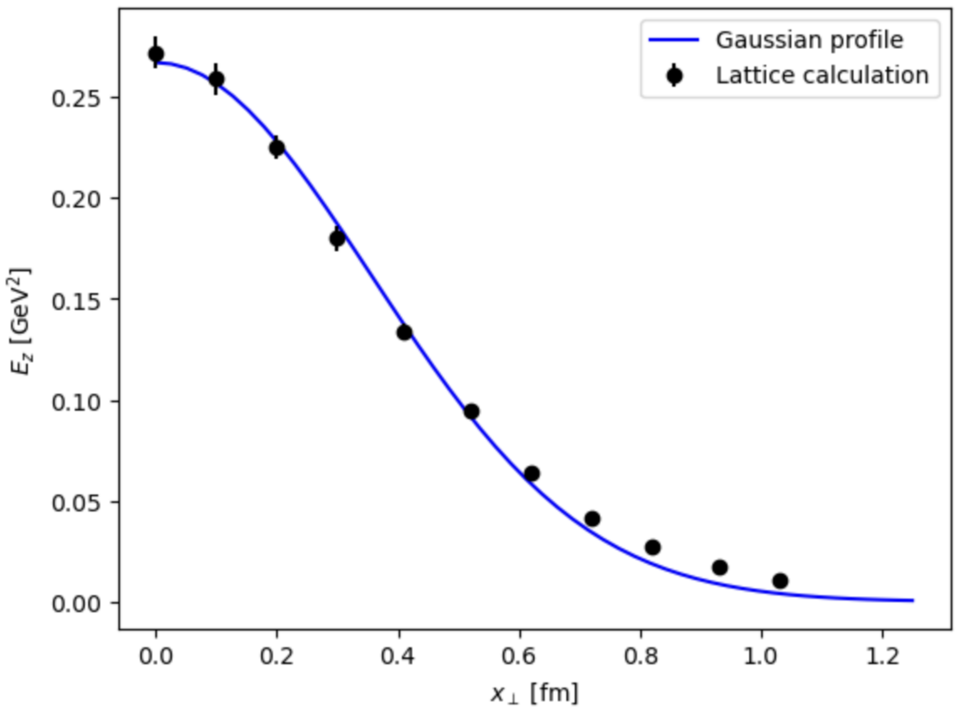

Figure 4: Calculated strength of color-electric field in z-direction, E_z, as function of the transverse distance from the flux tube axis. The figure also shows a Gaussian fit to the lattice points. Figure adapted from ref.[5]

In collisions that produce many hadrons, the strings will overlap and interact with each other. The strings overlapping means that the color-electric field is overlapping and, through superposition, the string tension will increase. The string shoving model [1] describes how the strings will behave when interacting. In this model, the strings will repel each other with a force generated by the transverse field. The magnitude of the force is given by [4][5]

$$f(d_\perp) = \frac{dV}{dd_\perp} = \frac{g\kappa d_\perp}{R^2} \exp\left(-\frac{d_\perp^2}{4R^2}\right). \tag{2.7}$$

Here, $d_\perp$ is the distance between the centre of the strings and R is the equilibrium radius, which is when the string has expanded to a stable shape. g is the ratio of energy density in the color-electric field to the string tension and V is the potential energy of the string.

2.3 PYTHIA

PYTHIA is a program that generates high-energy collisions and simulates the hadronization process. It is based on the Lund fragmentation scheme, including string-breaking dynamic, transverse momentum kicks and momentum fragmentation distribution given by Equation (2.6). PYTHIA is a Monte Carlo event generator and simulates the full process from scattering to observable final-state particles. A hard scattering process is modelled before parton showers are generated. Partons are connected by color-flow and move on to the hadronization process, which is described by the Lund string model. The unstable particles decay until only stable particles are left. PYTHIA includes the string shoving mechanism, which is described in Section 2.2. Since the classical shoving force has the form of the derivative of a Gaussian, the quantum mechanical model below uses a Gaussian repulsive potential as an effective description of string overlap. In this thesis, PYTHIA is only used for string shoving and hadronization. The elliptic flow, v_2, is calculated with the string shoving framework in PYTHIA. The strings are places with a given transverse separation, R_{sep}, that ranges from 0 to 7 fm and the value of v_2 is calculated for many events.

2.4 2-site toy model in QM

As explained in the previous section, the strings have been treated as classical objects so far. Hadronization happens at length scales where quantum effects are dominant and it is therefore appropriate to treat the strings as quantum objects. The idea is to treat one single string, with wave function $\psi(x,t)$, that interacts with the potential, V, which comes from another string or multiplet. To understand the physics of the interaction, we start by considering a 2-site lattice [9]. The sites are labelled a_1 and a_2, defined as

$$|a_1\rangle = \begin{pmatrix}1\\0\end{pmatrix}, \qquad |a_2\rangle = \begin{pmatrix}0\\1\end{pmatrix}. \tag{2.8}$$

The wave function $\psi(x,t)$ is defined to start in $|a_1\rangle$ and a potential, V, is added to that state. The Hamiltonian of the system is [10]

$$H = \begin{pmatrix} V & -J \\ -J & 0 \end{pmatrix}, \tag{2.9}$$

By shifting the zero-point of energy, the Hamiltonian can be expressed as

$$H = \begin{pmatrix} \Delta & -J \\ -J & -\Delta \end{pmatrix}, \tag{2.10}$$

where $\Delta = \frac{V}{2}$. This is mathematically equivalent to a two-level system where the Rabi model [11] applies and the eigenvalues become

$$E_{\pm} = \pm\sqrt{J^2 + \Delta^2}. \tag{2.11}$$

The time evolution of the state becomes

$$|\psi(t)\rangle = \cos(\theta)e^{-iE_+t}|\phi_+\rangle - \sin(\theta)e^{-iE_-t}|\phi_-\rangle, \tag{2.12}$$

where the angle θ is defined as

$$\tan(2\theta) = \frac{J}{\Delta}. \tag{2.13}$$

The probability of the string being in site $|a_2\rangle$ is calculated to be

$$P(|a_2\rangle)(t) = \frac{J^2}{J^2 + \Delta^2}\sin^2\left(\sqrt{J^2 + \Delta^2}t\right). \tag{2.14}$$

The full derivation of $P(|a_2\rangle)$ is shown in Appendix A. The amplitude of $P(|a_2\rangle)(t)$ depends on the ratio Δ/J. Importantly, the probability to find the string in state $|a_2\rangle$ will vanish for large Δ/J. This suggests that, in a quantum mechanical description, increasing the effective potential can suppress mobility away from the initial configuration. In the string shoving model, this motivates studying if a higher density of overlapping strings can reduce or modify the classical response. The two-site model is not intended as a realistic string model, but as a minimal example showing how an energy offset can suppress the escape from the initial state.

3 Method

To investigate how the strings will behave in a quantum mechanical system, the Schrödinger equation needs to be solved. The aim is to find the probability distribution for the relative transverse separation of the strings by calculating $|\psi(x,t)|^2$. This is done in one dimension and two dimensions. In Section 3.1, the one-dimensional case provides the groundwork for the two-dimensional case. Section 3.2 shows the calculation of the relative separation of the strings in two dimensions. Additionally, in Section 3.3, the radial probability current is calculated to see how the system will evolve over time. To answer the main question posed in this thesis, the calculation of the elliptic flow is also explained in Section 3.4.

3.1 One-dimensional implementation

In the one-dimensional case, one string is fixed, defining the potential in the Schrödinger equation, while the other string is treated as a moving wave packet. To find the position of the moving string, the Schrödinger equation,

$$i\frac{\partial\psi(x,t)}{\partial t} = \left[-\frac{1}{2m}\nabla^2 + V(x)\right]\psi(x,t), \tag{3.1}$$

needs to be solved. Here, m is an effective inertial parameter that controls the transverse motion and should not be interpreted as a physical rest mass of the string. The value of m is set to 1 GeV. Natural units, where $\hbar = c = 1$ are used throughout the project and all results are given in femtometers. A non-relativistic approximation is chosen here. A relativistic treatment would be very complex and since the relative motion between the strings is slow, a non-relativistic approximation is reasonable. The equation needs to be solved for the full one-dimensional space and is solved numerically on a finite space domain.

The normalized wave packet of a string is defined as the Gaussian

$$\psi = \frac{1}{(\pi\sigma^2)^{1/4}}\exp\left(\frac{-(x-x_0)^2}{2\sigma^2}\right)\cdot\exp\left(ik_0x\right), \tag{3.2}$$

where x is the position and k_0 is the momentum of the string. This is done since the transverse profile of the strings' color-field is almost a Gaussian, as explained in Section 2.2, and the wave packet is made to mirror this shape. After giving the string an initial position and setting the boundary conditions, the Crank-Nicolson solver [12] was implemented to solve for ψ_k^{n+1} in

$$\mathbf{A}\psi_k^{n+1} = \Omega_k = \mathbf{B}\psi_k^n. \tag{3.3}$$

$\mathbf{A}$ and $\mathbf{B}$ contain the Hamiltonian, which contains the kinetic and potential energy of the strings, and they are defined as

$$\begin{aligned}\mathbf{A} &= \left(\mathbf{1} + \frac{i\Delta t}{2}\mathbf{H}\right), \\ \mathbf{B} &= \left(\mathbf{1} - \frac{i\Delta t}{2}\mathbf{H}\right).\end{aligned} \tag{3.4}$$

The elements of **A** and **B** are numerically calculated with recursion relations. The recursion relations for the elements in matrix **A** are defined as

$$\begin{aligned}a_1 &= 2\left(1 + \Delta x^2 V_1 - i\frac{2\Delta x^2}{\Delta t}\right), \\ a_k &= 2\left(2 + \Delta x^2 V_k - i\frac{2\Delta x^2}{\Delta t}\right) - \frac{1}{a_{k-1}}.\end{aligned} \tag{3.5}$$

Ω is first set equal to the RHS in the original matrix equation;

$$\Omega^n = \mathbf{B}\psi^n = \left(\mathbf{1} - i\frac{\Delta t}{2}\mathbf{H}\right)\psi^n. \tag{3.6}$$

The recursion relation for the RHS then becomes

$$\Omega_k^n = -\psi_{k-1}^n + \left(i \cdot 2\frac{\Delta x^2}{\Delta t} + 1 + \Delta x^2 V_k^n\right)\psi_k^n - \psi_{k+1}^n. \tag{3.7}$$

This also has to equal the LHS of the original equation;

$$\mathbf{A}\psi^{n+1} = \Omega, \tag{3.8}$$

which is how the elements of **A** are found. After the original equation is solved for one step, the RHS also has to go to the next step. The elements in matrix **B** are then defined as

$$b_k = \frac{b_{k-1}}{a_{k-1}} + \Omega_k. \tag{3.9}$$

Now, all parts needed to solve for ψ_k^{n+1} in Equation (3.3) are found and the final state of the string can be calculated. The boundary conditions are

$$\psi_0^n = \psi_N^n = 0, \quad \forall n. \tag{3.10}$$

Recall the one-dimensional treatment where one string is stationary and one is moving. The probability of the moving string being in position x becomes

$$\mathrm{P}(x,t) = |\psi(x,t)|^2. \tag{3.11}$$

The one-dimensional simulation is done over spatial grid $N = 1000$, spatial step $\Delta x = 0.1$ fm and the time step is set to $\Delta t = 0.02$ fm. $\psi(x,t)$ is normalized once, at $t = 0$, and norm conservation is monitored.

3.2 Two-dimensional implementation

Treating the string interaction as a three-dimensional problem would become very complex. The string shoving happens only in the transverse plane, meaning the problem can be reduced to a two-dimensional problem. The 2D case corresponds to the plane perpendicular to the string axis. The 2D motion also captures the elliptical flow, which is introduced in Section 3.4. Before moving to two dimensions, a one-dimensional case was implemented to help develop and test the numerical approach. The primary focus is the two-dimensional problem which is formulated as a two-body problem, where the interaction only depends on the relative separation between the strings.

The two-body Schrödinger equation with coordinates $\vec{r_1}$ and $\vec{r_2}$ is [9]

$$i\frac{\partial\psi(\vec{r_1},\vec{r_2},t)}{\partial t} = \left[-\frac{1}{2m_1}\nabla_1^2 - \frac{1}{2m_2}\nabla_2^2 + V(\vec{r_1}-\vec{r_2})\right]\psi(\vec{r_1},\vec{r_2},t). \tag{3.12}$$

The center of mass coordinate is introduced

$$\vec{R}_{CM} = \frac{m_1\vec{r_1}+m_2\vec{r_2}}{m_1+m_2} \quad \text{and} \quad \vec{r} = \vec{r_1}-\vec{r_2}, \tag{3.13}$$

where m_1 and m_2 are the effective inertial parameters assigned to the string.

To simplify the Schrödinger equation, the reduced mass is defined as

$$\mu = \frac{m_1 m_2}{m_1+m_2} = \frac{m_1 m_2}{M} = 0.1\text{GeV}, \tag{3.14}$$

where $M = m_1+m_2$. The value 0.1 GeV is chosen for explanatory purposes, it demonstrates the quantum effects and maintains numerical stability. Using the chain rule, the gradients are rewritten as

$$\nabla_1^2 = \left(\frac{m_1}{M}\nabla_{\vec{R}_{CM}} + \nabla_{\vec{r}}\right)^2 = \frac{m_1^2}{M^2}\nabla^2_{\vec{R}_{CM}} + \nabla^2_{\vec{r}} + 2\frac{m_1}{M}\nabla_{\vec{R}_{CM}}\cdot\nabla_{\vec{r}}, \tag{3.15}$$

$$\nabla_2^2 = \left(\frac{m_2}{M}\nabla_{\vec{R}_{CM}} - \nabla_{\vec{r}}\right)^2 = \frac{m_2^2}{M^2}\nabla^2_{\vec{R}_{CM}} + \nabla^2_{\vec{r}} - 2\frac{m_2}{M}\nabla_{\vec{R}_{CM}}\cdot\nabla_{\vec{r}}, \tag{3.16}$$

Using this, the Schrödinger Equation (3.12) is simplified to

$$i\frac{\partial\psi(\vec{r},t)}{\partial t} = \left[-\frac{1}{2\mu}\nabla^2_{\vec{r}} + V(\vec{r})\right]\psi(\vec{r},t), \tag{3.17}$$

where the RHS contains all the kinetic and potential energy of the strings. This equation can now be split into two equations

$$\begin{aligned} i\frac{\partial}{\partial t}\Phi(\vec{R}_{CM},t) &= -\frac{1}{2M}\nabla^2_{\vec{R}_{CM}}\Phi(\vec{R}_{CM},t), \\ i\frac{\partial}{\partial t}\psi(\vec{r},t) &= \left[-\frac{1}{2\mu}\nabla^2_{\vec{r}} + V(\vec{r})\right]\psi(\vec{r},t). \end{aligned} \tag{3.18}$$

As seen in these equations, it is the second equation that contains the information about the position of the strings. The full derivation of Equation (3.18) is shown in Appendix B. To solve for $\psi(\vec{r}, t)$ the numerical methods presented in the previous section need to be modified to include both x- and y-direction. The Alternating-direction implicit (ADI) method [13] is used since it can be applied directly to the Crank-Nicolson solver. The ADI method is an iterative method that can be used to solve equations of the form

$$AX - XB = C, \tag{3.19}$$

which has the same form as Equation (3.3). The x and y-coordinates are treated separately and give one-half of the solution each. First the x-derivative is taken implicitly and the y-derivative is taken explicitly, giving the following equation to be solved,

$$\left[\mathbf{1} + i\frac{\Delta t}{2}\left(-\frac{1}{2\mu}\frac{\partial^2}{\partial x^2} + \frac{V(x,y)}{2}\right)\right]\psi^{n+\frac{1}{2}} = \left[\mathbf{1} - i\frac{\Delta t}{2}\left(-\frac{1}{2\mu}\frac{\partial^2}{\partial y^2} + \frac{V(x,y)}{2}\right)\right]\psi^{n}. \tag{3.20}$$

Ω from Equation (3.7) is now re-defined to have an x-component and a y-component. The x-component becomes

$$\Omega_x = -\psi_{i-1,j}^{n+\frac{1}{2}} + 2\left[i \cdot 2\frac{\Delta x^2}{\Delta t} + 1 + \Delta x^2 V_{i,j}\right]\psi_{i,j}^{n+\frac{1}{2}} - \psi_{i+1,j}^{n+\frac{1}{2}}. \tag{3.21}$$

The elements a_k and b_k are re-defined in the same manner. After solving the x-components for a fixed y, the same process is repeated but now the y-derivative is taken implicitly and the x-derivative is taken explicitly. The x-update and y-update are applied sequentially to make the final solution, ψ^{n+1}, following the same steps as in the one dimensional case. Finally, the potential is defined as a Gaussian in two dimensions;

$$V(x,y) = V_0 \exp\left(\frac{-(x-x_0)^2 - (y-y_0)^2}{2\sigma^2}\right). \tag{3.22}$$

The same boundary conditions are defined as

$$\psi_{i,j}^{n} = 0 \quad \text{on the boundaries of the grid} \tag{3.23}$$

and the simulation is done over a 500×500 spatial grid. The spatial steps are set to $\Delta x = 0.1$ fm and the time step is set to $\Delta t = 0.1$ fm. The total probability $|\psi(x,y,t)|^2$ is made sure to equal 1 before the probability density is plotted over the spatial grid.

3.3 Near-region probability and probability current

To clarify how the strings move relative to each other when interacting some quantities can be calculated. The interaction region is defined as $r < R_{\text{int}}$ and the probability to be inside this region is

$$P_{\text{near}}(t) = \int_{r<R_{\text{int}}} |\psi(r,t)|^2 d^2r. \tag{3.24}$$

r is the relative distance between the centres of the strings interacting. $P_{\text{near}}(t)$ measures how much of the amplitude remains in the interaction region. This quantity can be considered over time for different parameters.

The methods in previous sections describe how to solve for the relative position of the strings. To find how the string is moving, the probability current is calculated. The probability current, $\vec{j}(r,t)$, is defined as

$$\frac{\partial}{\partial t}|\psi(r,t)|^2 + \nabla \cdot \vec{j}(r,t) = 0, \tag{3.25}$$

which becomes

$$\vec{j}(r,t) = \frac{1}{\mu}\text{Im}(\psi^*(r,t)\nabla\psi(r,t)). \tag{3.26}$$

To find the outgoing probability current, this is projected onto the outward radial direction, r. The radial probability current becomes

$$j_r(r,\theta,t) = \vec{j}(r,\theta,t) \cdot \hat{r}, \tag{3.27}$$

where θ is the relative angle between the relative momentum between the strings and the angle of $\vec{j}(r,t)$.

The wave function and probability current are computed on a Cartesian grid. The value of j_r, given at angle θ is obtained using bilinear interpolation. For each value of θ, the point $(x,y) = (R_{\text{int}}\cos(\theta), R_{\text{int}}\sin(\theta))$ is within a grid cell. The values of j_x and j_y of the four surrounding grid points are weighed by distance to the point and the interpolated components are computed. This is repeated for 360 angles between $-\pi$ and π. The radial component then becomes

$$j_r = j_x\cos(\theta) + j_y\sin(\theta). \tag{3.28}$$

3.4 Elliptic flow

When two strings interact, the interaction area will be elliptical. In such an interaction, the pressure gradient is larger along the minor axis. In small systems the momentum is increasing along the major axis, contradicting hydrodynamic predictions. This means that the elliptic flow, v_2, is negative [6]. v_2 is related to the distribution of particles along the azimuthal angle, ϕ, by

$$\frac{dN}{d\phi} \propto 1 + 2v_2\cos(2(\phi - \Psi)). \tag{3.29}$$

Here, ϕ is the direction of outgoing particles in the transverse plane and Ψ is the minor axis. The setup is shown in Figure 5. In the quantum mechanical treatment, the angle of ϕ is modified to change the outgoing angle of the particles. v_2 is determined as the average of many events and can be expressed as

$$\langle v_2\rangle = \langle\cos(2(\phi_C - \phi_{QM} - \Psi))\rangle. \tag{3.30}$$

Here, ϕ_C is the original angle used in the classical case and ϕ_{QM} is the shift in angle that the quantum mechanical treatment introduces.

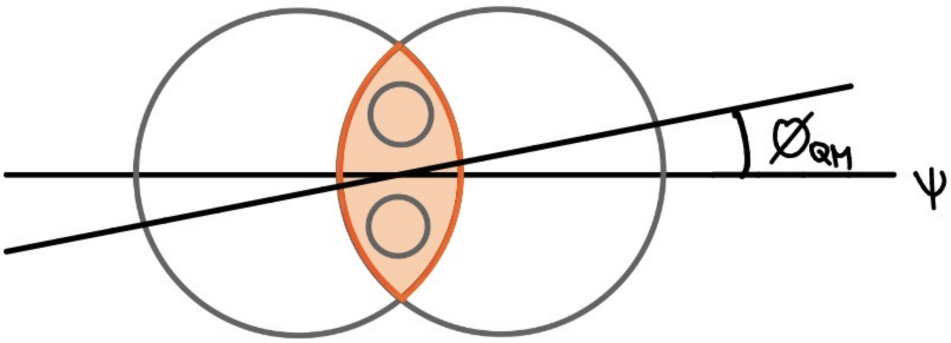

Figure 5: Representation of setup when calculating v_2. The elliptical interaction region is highlighted in orange. The minor axis, Ψ, and the angle ϕ_{QM} are shown.

4 Results

This section presents the results obtained from solving the Schrödinger equations using the method explained in Sections 3.1 and 3.2. The position of the string is found in one dimension, showing how the string will behave when treated quantum mechanically. The one dimensional case shows the results for different ratios of E_k/V, where E_k is kinetic energy of the string calculated as $E_k = k^2/2m$. Then, the positions of the strings in two dimensions is found as a probability distribution over space. The radial probability current is also calculated at the time of hadronization. From this, the elliptic flow is calculated and can be compared to the results in the classical case.

4.1 Lund strings in one dimension

The probability to find the string at a given position, x, is defined as $|\psi(x)|^2$ and is plotted over space, x, for different times, t. $\psi(x)$ is calculated by numerically solving Equation (3.3). The results are shown in Figures 6 and 7, together with the potential.

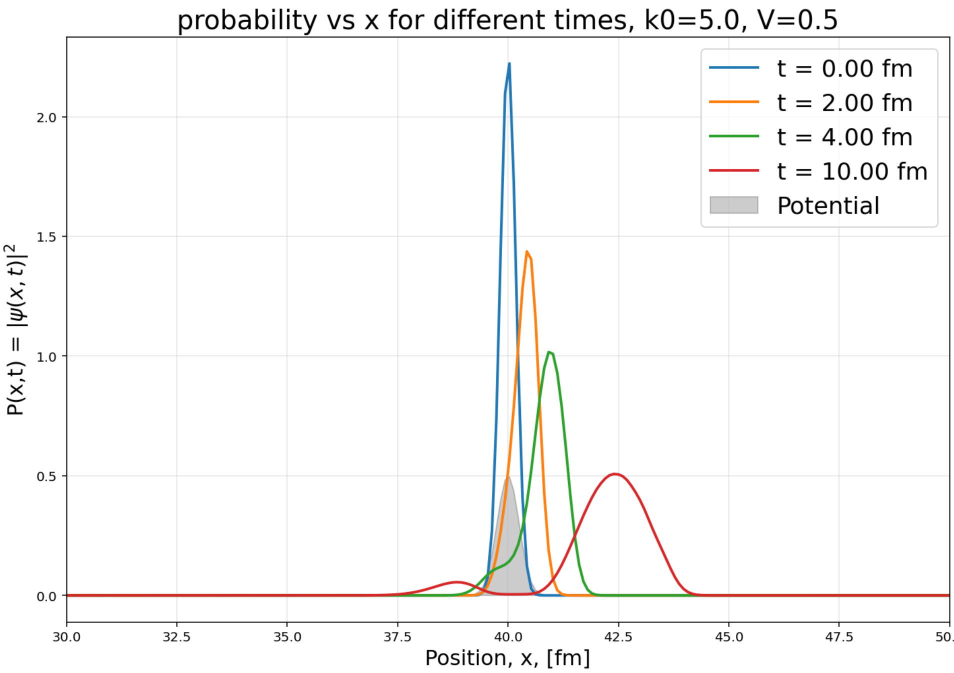

Figure 6: Figure of $|\psi(x,t)|^2$ over x for values $k_0 = 5.0$ GeV and $V = 0.5$ GeV.

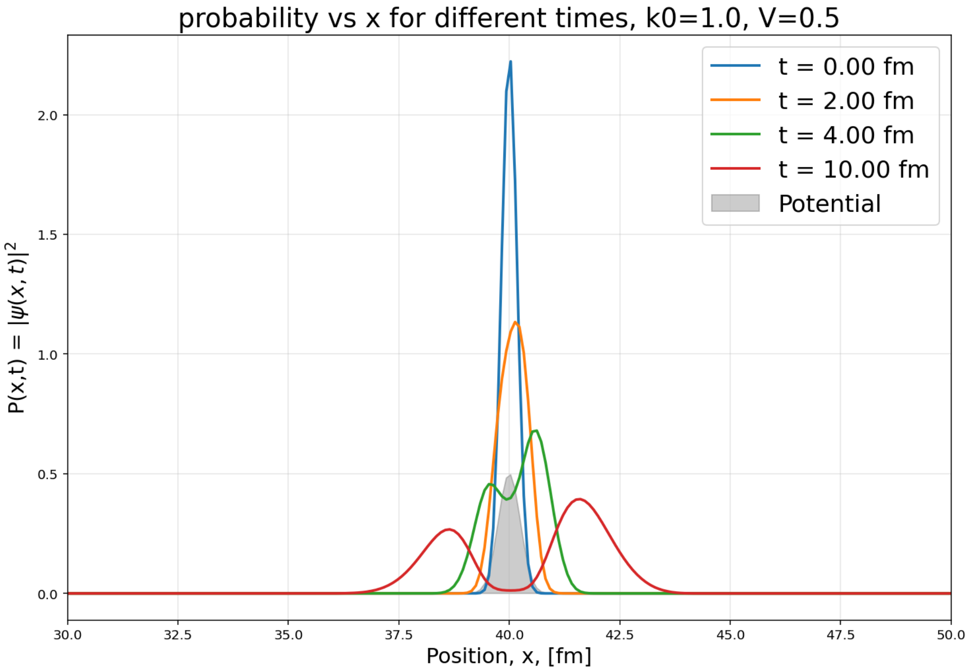

Figure 7: Figure of $|\psi(x,t)|^2$ over x for values $k_0 = 1.0$ GeV and $V = 0.5$ GeV.

The blue line is the initial state of the wave packet, defined to start on top of the potential barrier to simulate two strings on top of each other. Figures 6 and 7 also show the wave packet at later times. The momentum of the string, k_0, is defined to go in the positive x-direction. Due to the wave packet having a non-zero momentum the probability to move forward is non-zero. As a part of the wave packet is transmitted through the potential, a part of it will be reflected in the opposite direction. This is seen in both Figure 6 and 7 as the probability before the potential is non-zero after 10 fm.

In Figure 6, the plot shows the results for the momentum $k_0 = 5.0$ GeV and the ratio $E_k/V = 50$. Figure 7 shows the results for the momentum $k_0 = 1.0$ GeV and the ratio $E_k/V = 2.0$. When the kinetic energy of the wave packet is much larger than the potential, the wave packet can escape the potential. Since the wave packet represents the relative motion between the strings, the moving string remains near the interaction region for longer times when the momentum is small. The one-dimensional case is a natural evolution of the two-site model introduced in Section 2.4, extending from the discrete state transitions to an almost continuous space. These results are consistent with the two-site model where a large potential suppresses transitions away from the initial configuration.

4.2 Lund strings in 2D

Solving the Schrödinger equation in two dimensions results in a probability distribution of $|\psi(x,y)|^2$. The results for the same parameters as in the one-dimensional case are presented first. The result for $t = 0$ fm and $t = 1$ fm are shown in Figures 8 and 9. The blue area is the potential, which would correspond to the gray potential in the one-dimensional case. The orange part shows the probability to find the wave packet at each position. The plots show how the probability distribution of the relative position of the strings evolves over time.

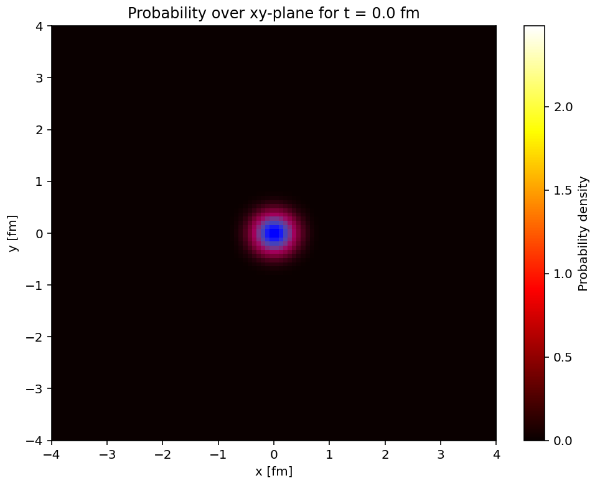

(a) Wave packet and potential for $t = 0$ fm and $E_k/V = 50$.

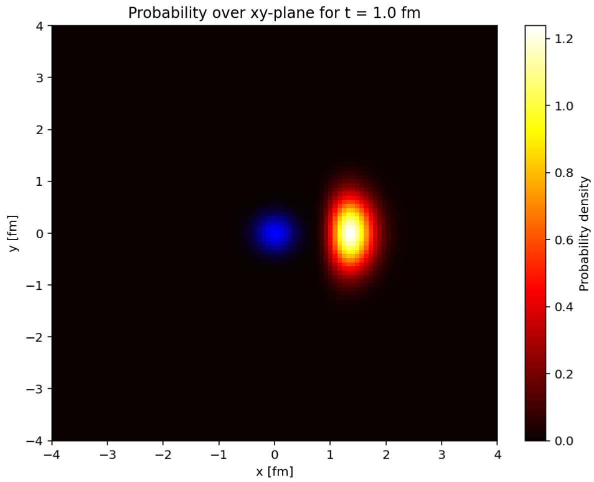

(b) Wave packet and potential for $t = 1$ fm and $E_k/V = 50$.

Figure 8: Figure of the distribution of $|\psi(x,y)|^2$ over xy-plane for $t = 0$ fm and $t = 1$ fm. The potential V is shown as a blue Gaussian and the probability density is given by the bar presented with each plot. Figures show the result for ratio $E_k/V = 50$.

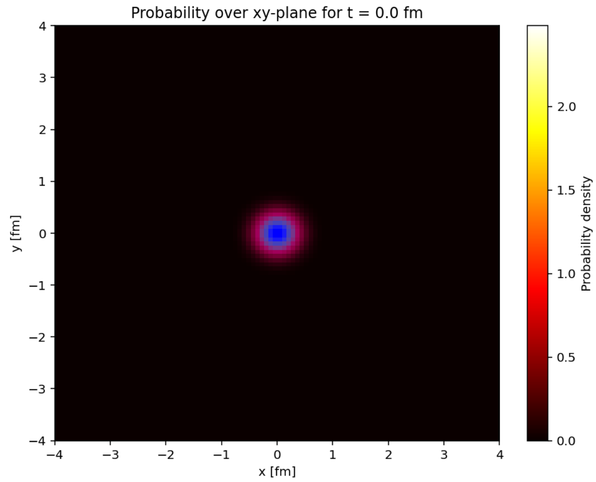

(a) Wave packet and potential for $t = 0$ fm and $E_k/V = 2$.

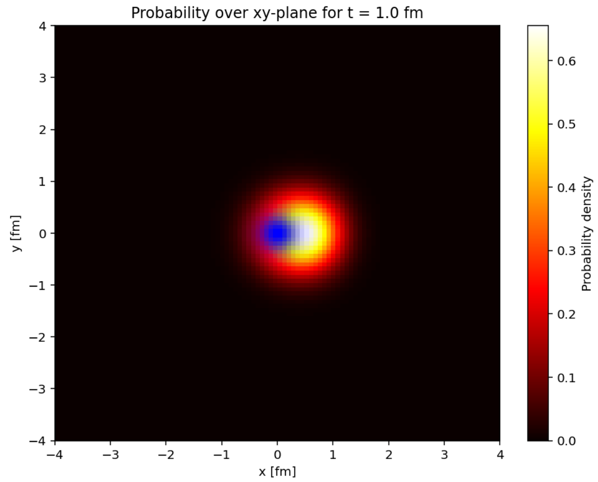

(b) Wave packet and potential for $t = 1$ fm and $E_k/V = 2$.

Figure 9: Figure of the distribution of $|\psi(x, y)|^2$ over xy-plane for $t = 0$ fm and $t = 1$ fm. The potential V is shown as a blue Gaussian and the probability density is given by the bar presented with each plot. Figures show the result for ratio $E_k/V = 2.0$.

As in the one-dimensional case, the relative momentum, $\vec{k}$, is defined in the positive x-direction and the results are plotted for the ratios $E_k/V = 50$ and $E_k/V = 2$. Figure 8 has the ratio $E_k/V = 50$ and the strings start directly on top of each other. The right plot shows the results after 1 fm, where the wave packet will easily escape the potential and move in the direction of $\vec{k}$. In Figure 9, $E_k/V = 2$ and the wave packet does not fully leave the potential and the probability to find the wave packet in and around the potential is non-zero. This is the same result as seen in Figures 6 and 7 in the previous section.

It is now possible to see that the probability of where to find the string is not only in the direction of the momentum. The probability will broaden along the y-axis, as seen in the plots for $t = 1$ fm. Part of this broadening is due to the natural spreading of a wave packet over time. However, this shows that treating the strings as quantum objects does change their interaction. In fact, the probability distribution appears to follow an approximately Gaussian shape around the direction of $\vec{k}$. The radial probability current is calculated to show this in the next section.

4.3 Interaction at characteristic hadronization time scale

For the next part, we want to focus on the state of the strings at time $t = 1.41$ fm. The strings will interact until they break. The actual breaking time follows the distribution in Equation (2.3). Rather than using the full distribution, we take the average value of τ, given in Equation (2.5), as a characteristic time scale for the hadronization. The results are studied for different values of $\vec{k}$, displacement $\vec{d}$ between the strings and radius R_{int}. R_{int} is the radius used in Equation (3.27) to calculate the radial probability current, which is plotted over the relative angle between $\vec{j}$ and $\vec{k}$. The results for $\vec{k} = 0.1$ GeV are shown in Figure 10.

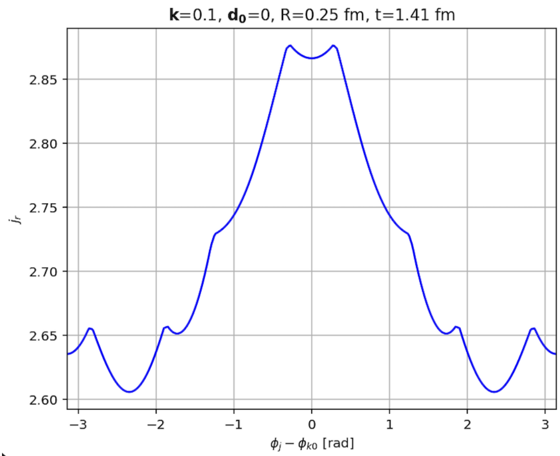

(a) Radial probability current over the relative angle between the probability current and the momentum for $\vec{k} = 0.1$ GeV, $\vec{d} = 0$ fm and $R_{\text{int}} = 0.25$ fm.

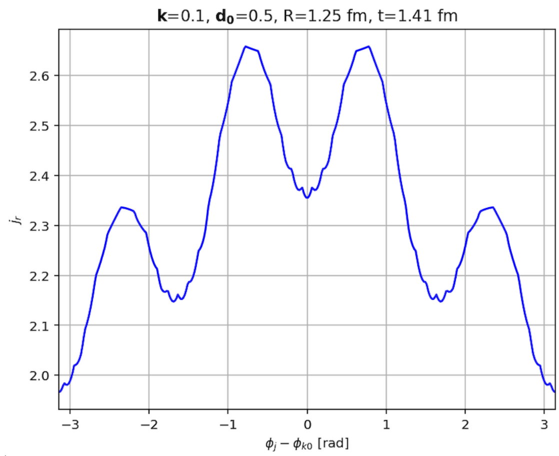

(b) Radial probability current over the relative angle between the probability current and the momentum for $\vec{k} = 0.1$ GeV, $\vec{d} = 0$ fm and $R_{\text{int}} = 1.25$ fm.

Figure 10: Figure of the radial probability current plotted over the relative angle between $\vec{j}$ and $\vec{k}$, for the different radii $R = 0.25$ fm and $R_{\text{int}} = 1.25$ fm.

In Figure 10, the left plot shows the radial probability current for $R_{\text{int}} = 0.25$ fm and the right plot shows it for $R_{\text{int}} = 1.25$ fm. The left figure shows one peak, which follows an almost Gaussian distribution around angle 0. The right figure shows peaks at angles $\pm\frac{\pi}{4}$ and $\pm\frac{3\pi}{4}$, with some noise. This means that the probability distribution of $|\psi(x, y)|^2$ changes at different distances from the interaction region. Considering one moving string in this two-body system, it will first move along the x-axis. At later times, the extracted radial current develops a multi-peak angular structure in a cross-like pattern at large r.

However, it should be noted that the extraction of the radial current relies heavily on the bilinear interpolation and angular sampling described in Section 3.3. This structure should therefore be interpreted with care as it depends on the grid resolution and the spatial step size in the calculations. The calculations in two dimensions are done using the ADI method described in Section 3.2, and it is important to note that the angular structure may also depend on the numerical method used. My implementation uses a square grid and it should be studied how a different shape grid may alter the multi-peak structure in Figure 10.

These patterns are translated to which direction the strings will move relative to each other. Sketches of how one string will move relative to a stationary string are shown in Figure 11, where the arrows are the most likely directions that the string will move and the strings are directly on top of each other. This shows that the strings will not only move away from each other in opposite directions, as in the classical case.

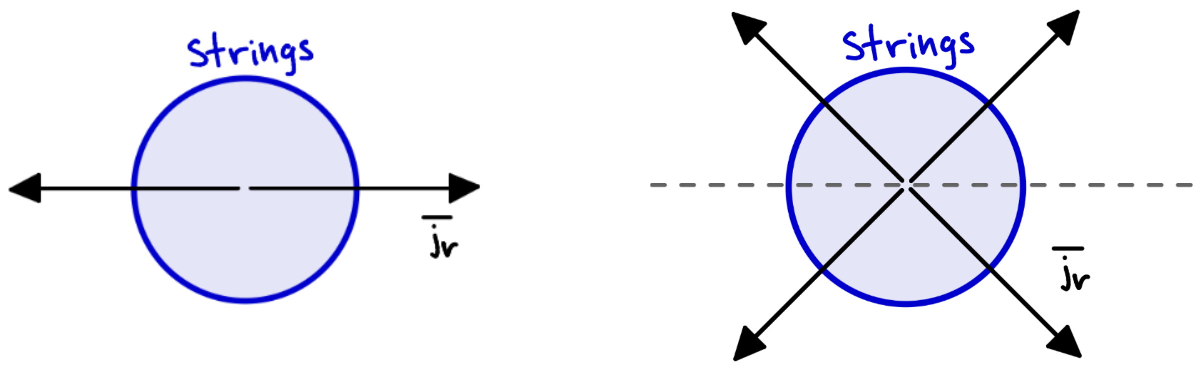

(a) Figure showing the direction of radial probability current for $\vec{k} = 0.1$ GeV and $R_{\text{int}} = 0.25$ fm.

(b) Figure showing the direction of radial probability current for $\vec{k} = 0.1$ GeV and $R_{\text{int}} = 0.75$ fm.

Figure 11: Schematic representation of cross-like current peak interpretation for $R_{\text{int}} = 0.25$ fm and $R_{\text{int}} = 0.75$ fm.

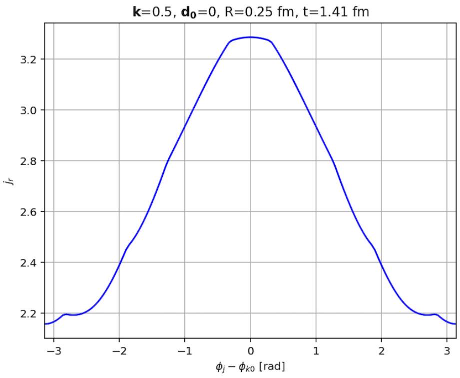

(a) Figure showing the direction of radial probability current for $\vec{k} = 0.5$ GeV and $R_{\text{int}} = 0.25$ fm.

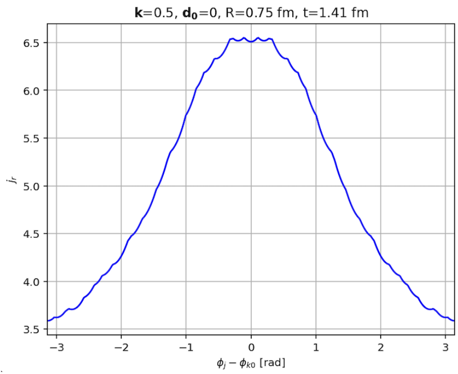

(b) Figure showing the direction of radial probability current for $\vec{k} = 0.5$ GeV and $R_{\text{int}} = 0.75$ fm.

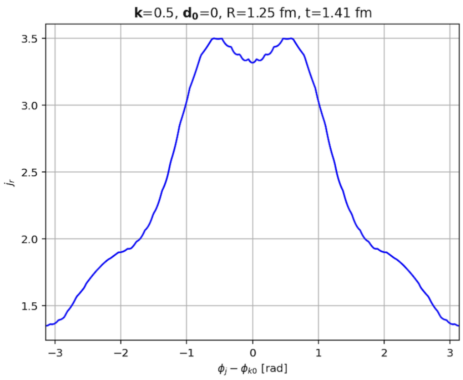

(c) Figure showing the direction of radial probability current for $\vec{k} = 0.5$ GeV and $R_{\text{int}} = 1.25$ fm.

Figure 12: Figure of the radial probability current plotted over the relative angle between $\vec{j}$ and $\vec{k}$, for values $R_{\text{int}} = 0.25$ fm, $R_{\text{int}} = 0.75$ fm and $R_{\text{int}} = 1.25$ fm.

When increasing $\vec{k}$ to 0.5 GeV, the radial probability current takes on a form that can be described by a Gaussian distribution around angle 0, before transitioning to the 'cross-like' pattern. The radial probability current for $\vec{k} = 0.5$ is shown in Figure 12. For $R_{\text{int}} = 0.25$ fm the radial probability current peaks around angle 0 and the string will move mainly in the direction of its momentum close to the interaction region. For $R_{\text{int}} = 0.75$ fm, the peak is broadening and starting to split into the peaks shown when $R_{\text{int}} = 1.25$ fm. Even further from the interaction region, the radial probability current is expected to peak at angles $\pm\frac{\pi}{4}$ and $\pm\frac{3\pi}{4}$ and look like the right plot in Figure 10. $\vec{j_r}$ will have this shape until it drops to oscillate with a very small amplitude, indicating that the string has not yet reached that distance. When increasing the momentum, $\vec{j_r}$ will follow a Gaussian-like distribution for larger R_{int}, since the momentum will be large enough for the wave packet to escape the potential and move in only the direction of $\vec{k}$. When $R_{\text{int}} = 1.25$ fm, it is clear that the probability current will transition to peak at angles $\pm\frac{\pi}{4}$ and $\pm\frac{3\pi}{4}$ again. The results in Figure 10 are for $\vec{d} = 0$, but the results do not change when the value of $\vec{d}$ is increased. Figure 13 shows the results for when $\vec{d} = 1.0$ fm and the results appear to be the same as those in Figure 10.

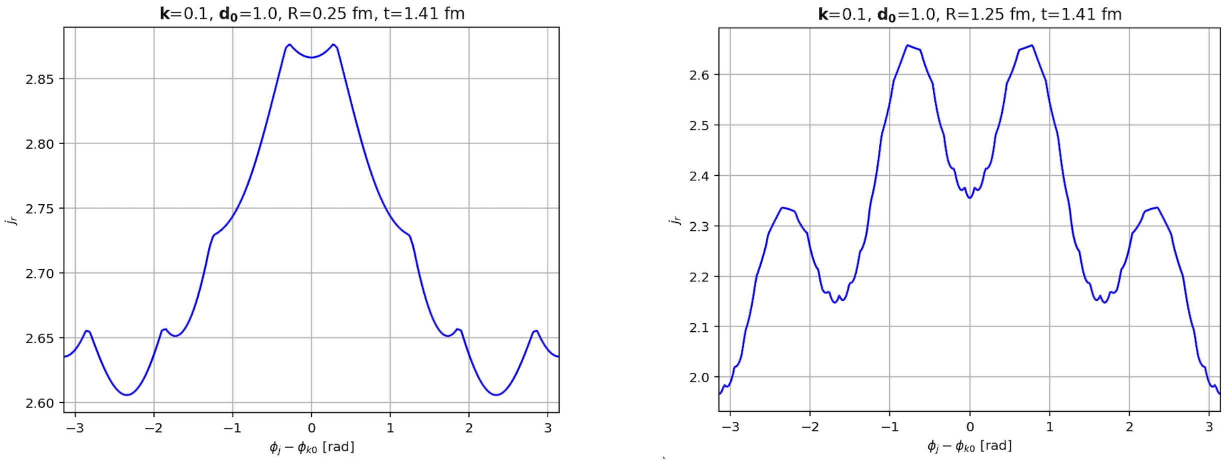

(a) Figure showing the direction of radial probability current for $\vec{k} = 0.1$ GeV, $\vec{d} = 1.0$ fm and $R_{\text{int}} = 0.25$ fm.

(b) Figure showing the direction of radial probability current for $\vec{k} = 0.1$ GeV, $\vec{d} = 1.0$ fm and $R_{\text{int}} = 1.25$ fm.

Figure 13: Figure of the radial probability current plotted over the relative angle between $\vec{j}$ and $\vec{k}$, for values $R_{\text{int}} = 0.25$ fm and $R_{\text{int}} = 1.25$ fm.

4.4 Calculating v_2

In Section 4.3, it is shown that the strings will move with some angular uncertainty. The angular distribution follows a Gaussian, in some cases, and the width is given by the full width half maximum (FWHM). The FWHM of the distribution in Figure 12 is calculated to be 2.7681 radians. The corresponding standard deviation is given by

$$\sigma = \frac{\text{FWHM}}{2\sqrt{2\ln(2)}}. \tag{4.1}$$

This σ defines the width of the Gaussian distribution which the angle ϕ_{QM} is randomly sampled from. This is the value that is used as ϕ_{QM} in Equation (3.30) to calculate v_2, since this describes how the strings move near the interaction region at the time of hadronization. v_2 is calculated for 1,000,000 events and the distribution is shown in Figure 14. v_2 is calculated for $R_{\text{sep}} = 0.25$ fm. This is not a full calculation of v_2, but an illustrative estimate of how angular smearing would affect v_2 with realistic hadronization.

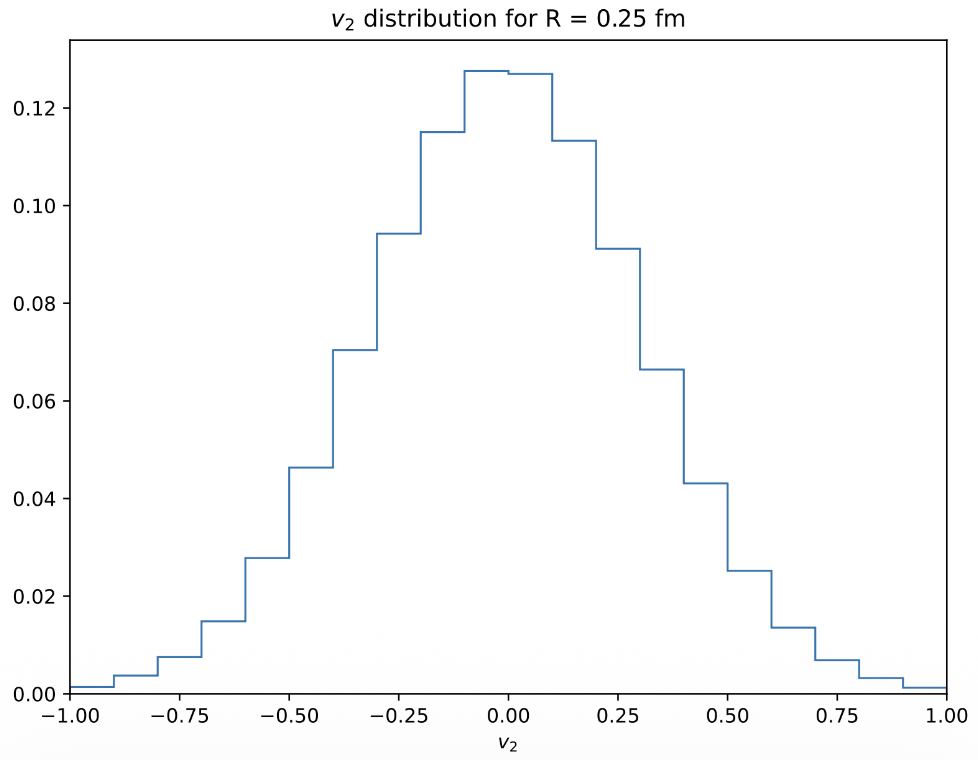

Figure 14: v_2 distribution for $R_{\text{sep}} = 0.25$ fm and 1000 000 events. The figure shows the distribution of v_2 with string shoving.

The process is repeated and v_2 is calculated for many values of R_{sep}. The distribution of v_2 has a single peak with a finite width in both cases because of the random momentum kicks described in Equation (2.4). The quantum mechanical effects will only change the amplitude of v_2.

The mean value $\langle v_2 \rangle$ is calculated for each value of R_{sep}, using Equation (3.30) and shown in Figure 15. Figure 15 shows the value of $\langle v_2 \rangle$ over R_{sep} with no string shoving and with string shoving when there is no angular spreading. As expected, the values of $\langle v_2 \rangle$ are zero when there is no string shoving. When including string shoving and the width is zero, meaning no quantum effects are present, the value of $\langle v_2 \rangle$ drops to almost -0.08 and then goes to zero for larger R_{sep}. This is the known result for this setup in the absence of quantum effects.

Figure 16 shows $\langle v_2 \rangle$ over R_{sep} when applying the quantum mechanical effects derived in the previous section. The plot includes the results for widths $0.5, 1.0$ and 2.7681 radians. The results for widths 0.5 and 1.0 radians are included to show how the amplitude of v_2 will decrease when increasing the distribution from which ϕ is chosen. As seen in Figure 16, the values of $\langle v_2 \rangle$ go to zero quickly when increasing the width and will be very close to zero for the width 2.7681 rad. This behaviour is expected as the distribution from which ϕ is chosen becomes so large that the average in Equation (3.30) goes to zero.

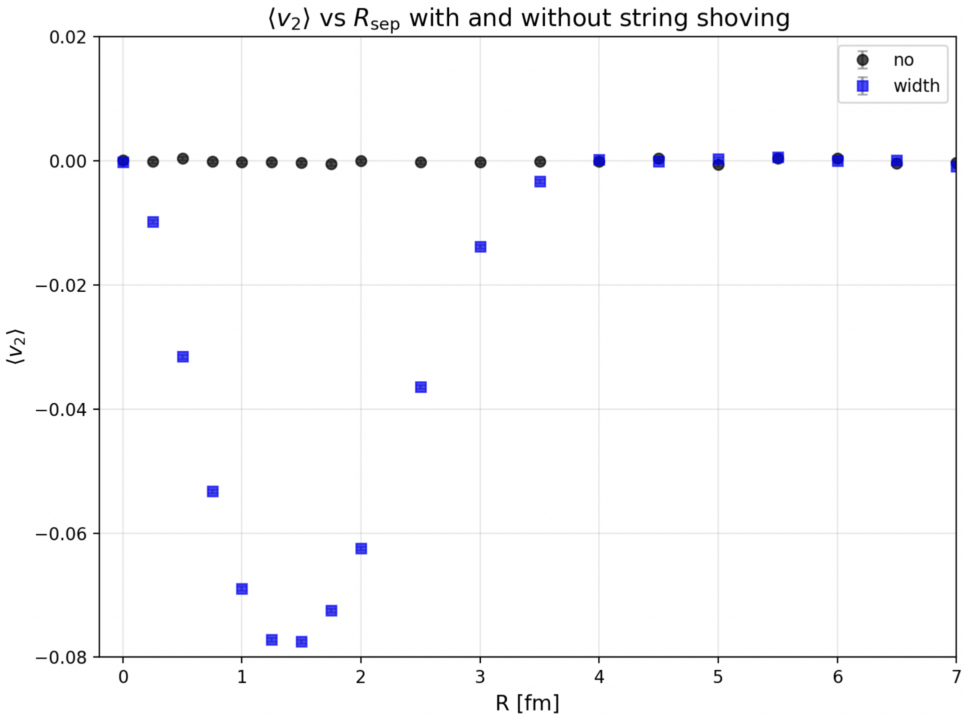

Figure 15: The calculated values of average $\langle v_2 \rangle$ over R_{sep} when there is no string shoving and when there is string shoving and the width is zero.

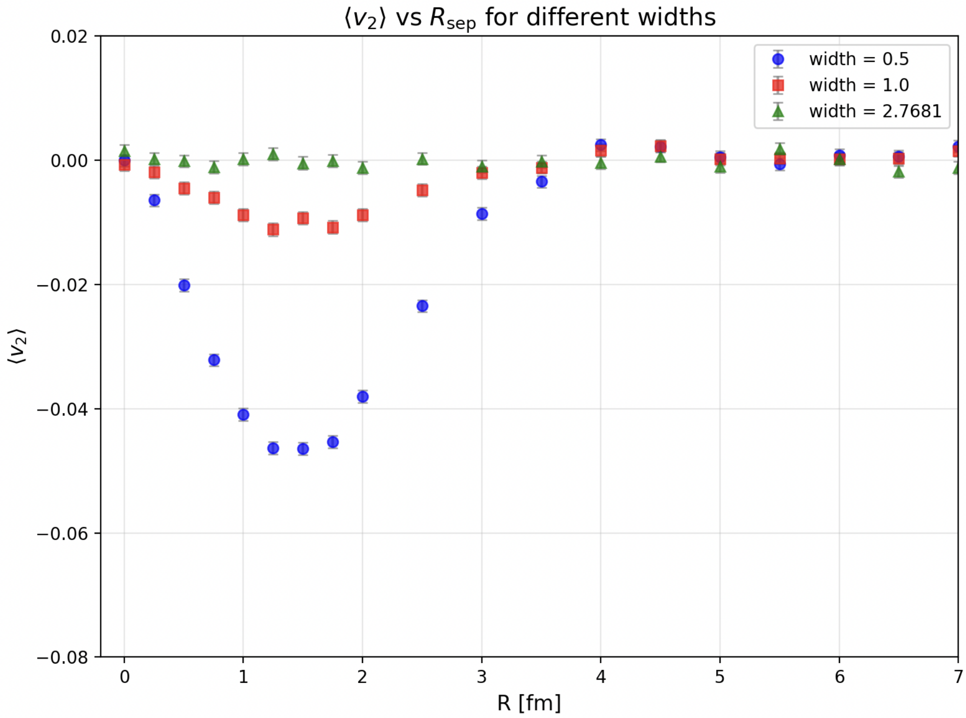

Figure 16: The calculated average $\langle v_2 \rangle$ over R_{sep} for widths $0.5, 1.0, 2.7681$ radians.

The value of $\langle v_2 \rangle$ is calculated by simulating 1000 000 events to minimize the uncertainties. For each value of R_{sep}, the error of $\langle v_2 \rangle$ is calculated and the values are very small. The errors are of order 0.0001 and are seen in Figure 15. There are limitations to the calculation of v_2 that should be noted. The value of σ, which gives the angular distribution that the quantum mechanical treatment introduces, is calculated from the radial probability current. The radial probability current is assumed to be a Gaussian distribution, which is an approximation. The calculations in PYTHIA are also made in a simplified setup of a two-string geometry. The value of v_2 may not apply to more complex systems. These limitations imply that the results in this section should be taken as a qualitative representation and not precise predictions.

5 Conclusion

This thesis analyzes how strings that are created in the hadronization process will behave in a quantum mechanical treatment. Within the simplified model, results indicate that a quantum treatment can modify the classical picture. The strings are analyzed at different times after interaction in both one and two dimensions. The results are presented as a probability distribution and a radial probability current over space, for different relative momentum $\vec{k}$ between the strings. The probable direction of the string motion is studied for different distances R_{int} from the interaction region. The angular direction of the strings' movement will evolve from a single peak to a multi-peak angular structure, that should be further investigated. This behaviour deviates from the classical predictions of the Lund string model, which states that the strings will move along a straight line. The produced elliptic flow with the quantum mechanical effects is compared to the classical values of v_2. $\langle v_2 \rangle$ is plotted over different values of R_{sep} where it is suggested that the magnitude of v_2 decreases when the angular distribution, that the quantum mechanical treatment introduces, increases.

While this thesis demonstrates that a quantum mechanical treatment of string interactions leads to angular uncertainty in the string motion, some limitations should be acknowledged. The analysis is restricted to a simplified system of only two strings in one and two dimensions. A more realistic system would include many overlapping strings in three dimensions. The strings are also treated in a non-relativistic approximation. This approximation is motivated by the slow relative motion of the strings, however a relativistic treatment would be more accurate. Additionally, all analyses are based on simplified models. The one-dimensional and two-dimensional solutions of the strings' interaction are based on the two-site toy model. The PYTHIA implementation used here employs a simplified two-string model setup. Finally, systematic uncertainties arising from using a discrete grid and bilinear interpolation should be considered. When estimating the value of v_2 in a quantum mechanical treatment, the results are not intended to be precise quantitative predictions.

Future work should address these limitations by extending the study to include many strings in three dimensions. A relativistic treatment would change the method of finding the strings' trajectories, but would be more realistic. Implementing the quantum effect in PYTHIA in the future would give new conclusions about the quantum mechanical treatment of Lund strings.

A Full derivation of 2-site model

Consider a two-site lattice, labelled a_1 and a_2;

$$|a_1\rangle = \begin{pmatrix} 1 \\ 0 \end{pmatrix}, \qquad |a_2\rangle = \begin{pmatrix} 0 \\ 1 \end{pmatrix}. \tag{A.1}$$

The wave function $\psi(x,t)$ is defined to start in $|a_1\rangle$. When there is no potential, the Hamiltonian of the system is

$$H = \begin{pmatrix} 0 & -J \\ -J & 0 \end{pmatrix}. \tag{A.2}$$

where the energy eigenvalues are $E_\pm = \pm J$. The normalized eigenstates become

$$\begin{aligned} |\phi_1\rangle &= \frac{1}{\sqrt{2}} \left(|a_1\rangle + |a_2\rangle \right), \\ |\phi_2\rangle &= \frac{1}{\sqrt{2}} \left(|a_1\rangle - |a_2\rangle \right). \end{aligned} \tag{A.3}$$

The initial state is

$$|\psi(0)\rangle = \frac{1}{\sqrt{2}} \left(|\psi_1\rangle + |\psi_2\rangle \right), \tag{A.4}$$

and the time evolution of the state is

$$\begin{aligned} |\psi(t)\rangle = \frac{1}{\sqrt{2}} \left(e^{iJt}|\phi_1\rangle + e^{-iJt}|\phi_2\rangle \right) = \\ \frac{1}{2} \left(e^{iJt}|a_1\rangle + e^{iJt}|a_2\rangle + e^{-iJt}|a_1\rangle - e^{-iJt}|a_2\rangle \right) \\ \frac{e^{iJt} + e^{-iJt}}{2}|a_1\rangle + \frac{e^{iJt} - e^{-iJt}}{2}|a_2\rangle \\ = \cos(Jt)|a_1\rangle + i\sin(Jt)|a_2\rangle. \end{aligned} \tag{A.5}$$

The probability to find the string in $|a_2\rangle$ is

$$\begin{aligned} P(|a_2\rangle) &= |\langle a_2|\psi(t)\rangle|^2 \\ &= |i\sin(Jt)|^2 = \sin^2(Jt), \end{aligned} \tag{A.6}$$

which shows that the system will oscillate between the states with frequency given by the energy J. When adding a potential V to $|a_1\rangle$ the Hamiltonian of the system becomes

$$H = \begin{pmatrix} V & -J \\ -J & 0 \end{pmatrix}, \tag{A.7}$$

where the normalized eigenstates are

$$|\phi_\pm\rangle = \frac{1}{\sqrt{1+\frac{J^2}{E_\pm^2}}} \cdot \begin{pmatrix} 1 \\ \frac{-J}{E_\pm} \end{pmatrix}. \tag{A.8}$$

By shifting the zero-point of energy, the Hamiltonian can be expressed as

$$H = \begin{pmatrix} \Delta & -J \\ -J & -\Delta \end{pmatrix}, \tag{A.9}$$

where $\Delta = \frac{V}{2}$. It is now a case where the Rabi model directly applies. The eigenvalues become

$$E_\pm = \pm\sqrt{J^2+\Delta^2}, \tag{A.10}$$

with eigenstates

$$|\phi_+\rangle = \begin{pmatrix} \cos(\theta) \\ \sin(\theta) \end{pmatrix}, \qquad |\phi_-\rangle = \begin{pmatrix} -\sin(\theta) \\ \cos(\theta) \end{pmatrix}. \tag{A.11}$$

The angle θ is defined as

$$\tan(2\theta) = \frac{J}{\Delta}. \tag{A.12}$$

The time evolution of the state becomes

$$|\psi(t)\rangle = \cos(\theta)e^{-iE_+t}|\phi_+\rangle - \sin(\theta)e^{-iE_-t}|\phi_-\rangle \tag{A.13}$$

and the probability of the string being in the $|a_2\rangle$ is calculated to be

$$\begin{aligned} P(|a_2\rangle)(t) = |\langle a_2|\psi(t)\rangle|^2 &= (\sin(\theta)\cos(\theta))^2 4\sin^2\left(\sqrt{J^2+\Delta^2}t\right) \\ &= \sin^2(2\theta)\sin^2\left(\sqrt{J^2+\Delta^2}t\right) = \frac{J^2}{J^2+\Delta^2}\sin^2\left(\sqrt{J^2+\Delta^2}t\right). \end{aligned} \tag{A.14}$$

The amplitude of $P(|a_2\rangle)(t)$ depends on the ratio Δ/J. $P(|a_2\rangle)$ is plotted over time, for different values of Δ/J, and shown in Figure 17.

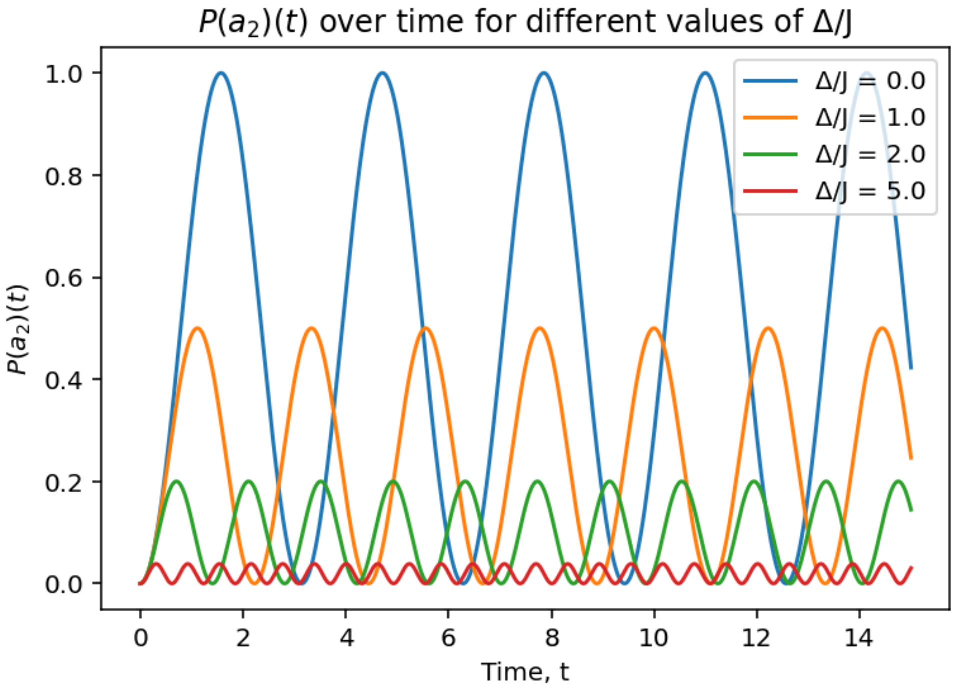

Figure 17: Plot of the probability of the string being found in $|a_2\rangle$ over time. The plot shows the results for different ratios of Δ/J.

Importantly, the probability to find the string in state $|a_2\rangle$ will vanish for large Δ/J.

B Full derivation of the Schrödinger equation in a 2-body system

The Schrödinger equation for a 2-body system with transverse coordinates $\mathbf{r_1}$ and $\mathbf{r_2}$ is

$$i\frac{\partial}{\partial t}\psi(\vec{r_1},\vec{r_2},t) = \left[-\frac{1}{2m_1}\nabla_1^2 - \frac{1}{2m_2}\nabla_2^2 + V(\vec{r_1}-\vec{r_2})\right]\psi(\vec{r_1},\vec{r_2},t) \tag{B.1}$$

The center of mass in introduced and defined as

$$\vec{R} = \frac{m_1\vec{r_1}+m_2\vec{r_2}}{m_1+m_2}, \vec{r} = \vec{r_1}-\vec{r_2}. \tag{B.2}$$

Additionally, the reduced mass is defined as

$$\mu = \frac{m_1 m_2}{m_1+m_2} = \frac{m_1 m_2}{M}. \tag{B.3}$$

The coordinates are inverted to find the coordinates

$$\begin{aligned} \vec{r_1} &= \vec{R} + \frac{m_2}{M}\vec{r}, \\ \vec{r_2} &= \vec{R} - \frac{m1}{M}\vec{r}. \end{aligned} \tag{B.4}$$

and gradients

$$\begin{aligned} \nabla_1 &= \frac{m_1}{M}\nabla_{\vec{R}+\nabla_{\vec{r}},} \\ \nabla_2 &= \frac{m_2}{M}\nabla_{\vec{R}-\nabla_{\vec{r}}.} \end{aligned} \tag{B.5}$$

Squaring the gradients gives

$$\begin{aligned} \nabla_1^2 &= \left(\frac{m_2}{M}\right)^2\nabla_{\vec{R}}^2 + \frac{2m_1}{M}\left(\nabla_{\vec{R}}\cdot\nabla_{\vec{r}}\right) + \nabla_{\vec{r}}^2, \\ \nabla_2^2 &= \left(\frac{m_2}{M}\right)^2\nabla_{\vec{R}}^2 - \frac{2m_2}{M}\left(\nabla_{\vec{R}}\cdot\nabla_{\vec{r}}\right) + \nabla_{\vec{r}}^2. \end{aligned} \tag{B.6}$$

Inserting this in the kinetic part of the Schrödinger equation yields

$$\begin{aligned} -\frac{1}{2m_1}\nabla_1^2 - \frac{1}{2m_1}\nabla_2^2 &= -\frac{1}{2m_1}\left[\left(\frac{m_1}{M}\right)^2\nabla_{\vec{R}}^2 + \frac{2m_1}{M}\left(\nabla_{\vec{R}}\cdot\nabla_{\vec{r}}\right)^2 + \nabla_{\vec{r}}^2\right] \\ &\quad -\frac{1}{2m_2}\left[\left(\frac{m_2}{M}\right)^2\nabla_{\vec{R}}^2 - \frac{2m_2}{M}\left(\nabla_{\vec{R}}\cdot\nabla_{\vec{r}}\right) + \nabla_{\vec{r}}^2\right] \\ &= -\frac{1}{2}\left[\left(\frac{m_1}{M}+\frac{m_2}{M}\right)\nabla_{\vec{R}}^2 + \left(\frac{1}{m_1}+\frac{1}{m_2}\right)\nabla_{\vec{r}}^2\right] \\ &= -\frac{1}{2}\left[\frac{1}{M}\nabla_{\vec{R}}^2 + \frac{1}{\mu}\nabla_{\vec{r}}^2\right]. \end{aligned} \tag{B.7}$$

The Schrödinger equation becomes

$$i\frac{\partial}{\partial t}\psi(\vec{R},\vec{r},t) = \left[-\frac{1}{2M}\nabla^2_{\vec{R}} - \frac{1}{2\mu}\nabla^2_{\vec{r}} + V(\vec{r})\right]\psi(\vec{R},\vec{r},t) \tag{B.8}$$

which can be split into the parts

$$\begin{aligned} i\frac{\partial}{\partial t}\Phi(\vec{R},t) &= -\frac{1}{2M}\nabla^2_{\vec{R}}\Phi(\vec{R},t) \\ i\frac{\partial}{\partial t}\psi(\vec{r},t) &= -\left[\frac{1}{2\mu}\nabla^2_{\vec{r}} + V(\vec{r})\right]\psi(\vec{r},t). \end{aligned} \tag{B.9}$$

References

[1] Christian Bierlich, Smita Chakraborty, Nishita Desai, Leif Gellersen, Ilkka Helenius, Philip Ilten, Leif Lönnblad, Stephen Mrenna, Stefan Prestel, Christian T. Preuss, Torbjörn Sjöstrand, Peter Skands, Marius Utheim, and Rob Verheyen. A comprehensive guide to the physics and usage of PYTHIA 8.3, 2022.

[2] Andy Buckley, Jonathan Butterworth, Stefan Gieseke, David Grellscheid, Stefan Höche, Hendrik Hoeth, Frank Krauss, Leif Lönnblad, Emily Nurse, Peter Richardson, Steffen Schumann, Michael H. Seymour, Torbjörn Sjöstrand, Peter Skands, and Bryan Webber. General-purpose event generators for LHC physics. *Physics Reports*, 504(5):145–233, 2011.

[3] Christian Bierlich, Gösta Gustafson, Leif Lönnblad, and Andrey Tarasov. Effects of Overlapping Strings in pp Collisions. *JHEP*, 03:148, 2015.

[4] Christian Bierlich, Smita Chakraborty, Gösta Gustafson, and Leif Lönnblad. Setting the string shoving picture in a new frame. *Journal of High Energy Physics*, 2021(3), March 2021.

[5] Christian Bierlich. String Interactions as a Source of Collective Behaviour. *Universe*, 10(1):46, 2024.

[6] Christian Bierlich, Peter Christiansen, Gösta Gustafson, Leif Lönnblad, Robin Törnkvist, and Korinna Zapp. Going against the flow: Revealing the QCD degrees of freedom in hadronic collisions. *Phys. Lett. B*, 874:140216, 2026.

[7] Nora Brambilla and Antonio Vairo. Quark confinement and the hadron spectrum. In *13th Annual HUGS AT CEBAF*, pages 151–220, 1999.

[8] Abdullah Guvendi and Omar Mustafa. An innovative model for coupled fermion-antifermion pairs. *Eur. Phys. J. C*, 84:866, 2024.

[9] David J. Griffiths and Darrell F. Schroeter. *Introduction to Quantum Mechanics*. Cambridge University Press, 3 edition, 2018.

[10] J. J. Sakurai and Jim Napolitano. *Modern Quantum Mechanics*. Cambridge University Press, Cambridge, 3rd edition, 2021.

[11] Christopher C. Gerry and Peter L. Knight. *Introductory Quantum Optics*. Cambridge University Press, Cambridge, 2005.

[12] Benjamin A. Stickler and Ewald Schachinger. *Basic Concepts in Computational Physics*. Springer, Cham, 2 edition, 2016.

[13] Eugene L. Wachspress. Trail to a Lyapunov equation solver. *Comput. Math. Appl.*, 55(8):1653–1659, April 2008.